

A polymer-free, biomimicry drug self-delivery system fabricated via synergistic combination of bottom-up and top-down approaches

Xiaobao Xu^{a,b,c}, Gaomai Yang^c, Xiangdong Xue^c, Hongwei Lu^c, Hao Wu^c, Yee Huang^d, Di Jing^c, Wenwu Xiao^c, Jingkui Tian^a, Wei Yao^b, Chong-xian Pan^b, Tzu-yin Lin^{b,*}, Yuanpei Li^{c,*}

^a College of Biomedical Engineering & Instrument Science, Zhejiang University, Hangzhou 310027, China

^b Department of Internal Medicine, University of California Davis, Sacramento, CA 95817, USA

^c Department of Biochemistry and Molecular Medicine, UC Davis Comprehensive Cancer Center, University of California Davis, Sacramento, CA 95817, USA

^d Institute of Animal Husbandry and Veterinary Science, Zhejiang Academy of Agricultural Sciences, Hangzhou, Zhejiang 310021, China

Corresponding authors: YP Li, T-Y Lin

2700 Stockton Blvd

Sacramento CA

95817

*Email: lypli@ucdavis.edu; tylin@ucdavis.edu

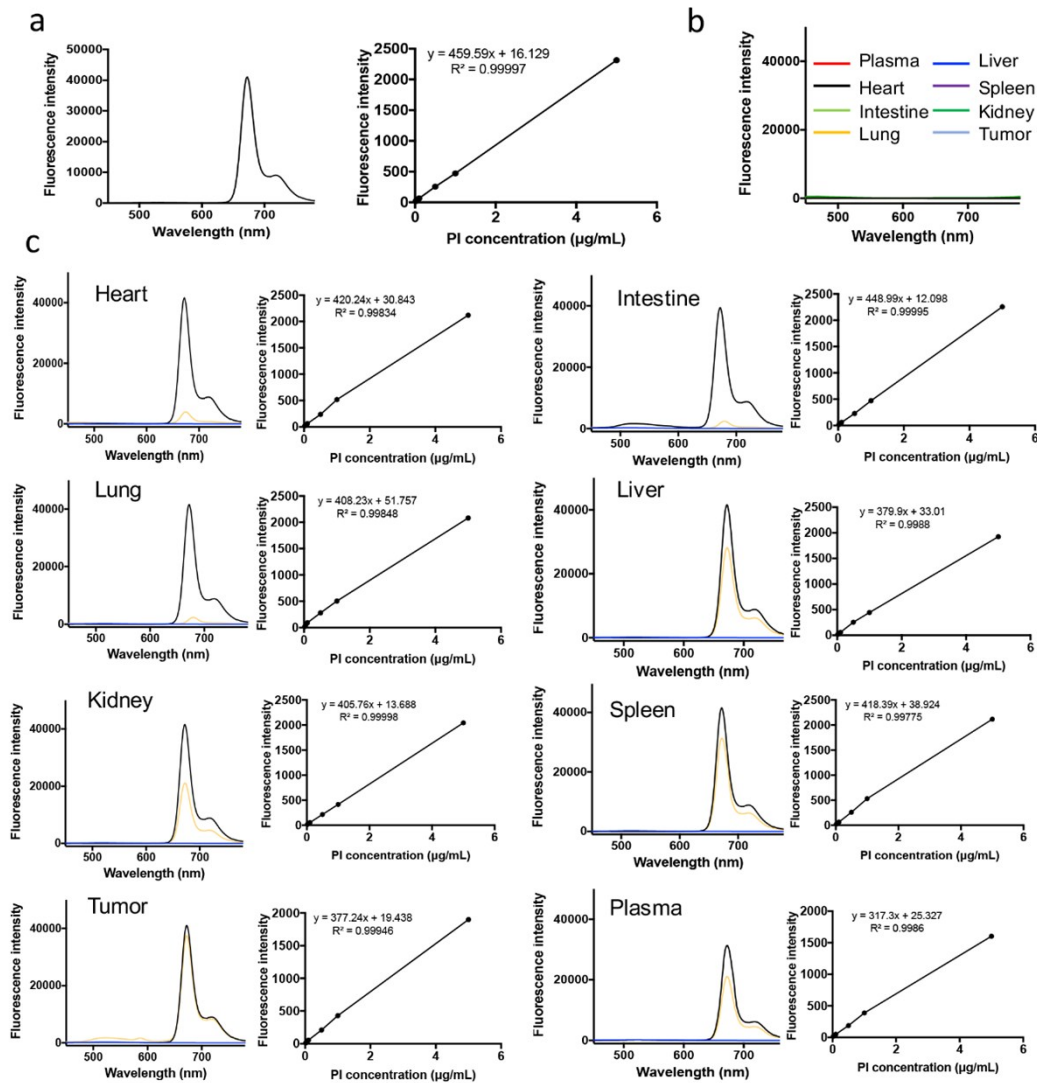


Figure S1 a) Fluorescence spectra (412 nm excitation) and dilution/intensity curves for RBC-PI prior injection in methanol. b) Fluorescence spectra (412 nm excitation) of background signal emitted from intact homogenized organs and plasma. Tissue/serum collected from animals without PI administration were homogenized in the PBS. Proteins were precipitated by 5 times methanol. Supernatant was dried and samples were then re-dissolved with pure methanol. Of note, there were minimal signals in all organs. c) Fluorescence spectra (412 nm excitation) (dark line) and standard curve with spiked RBC-PI generated from organs without biological matrix and fluorescence

spectra of samples from the same organs after RBC-PI injection (Yellow line). Blue line represent of the spectra background signal emitted from intact homogenized organs and plasma.

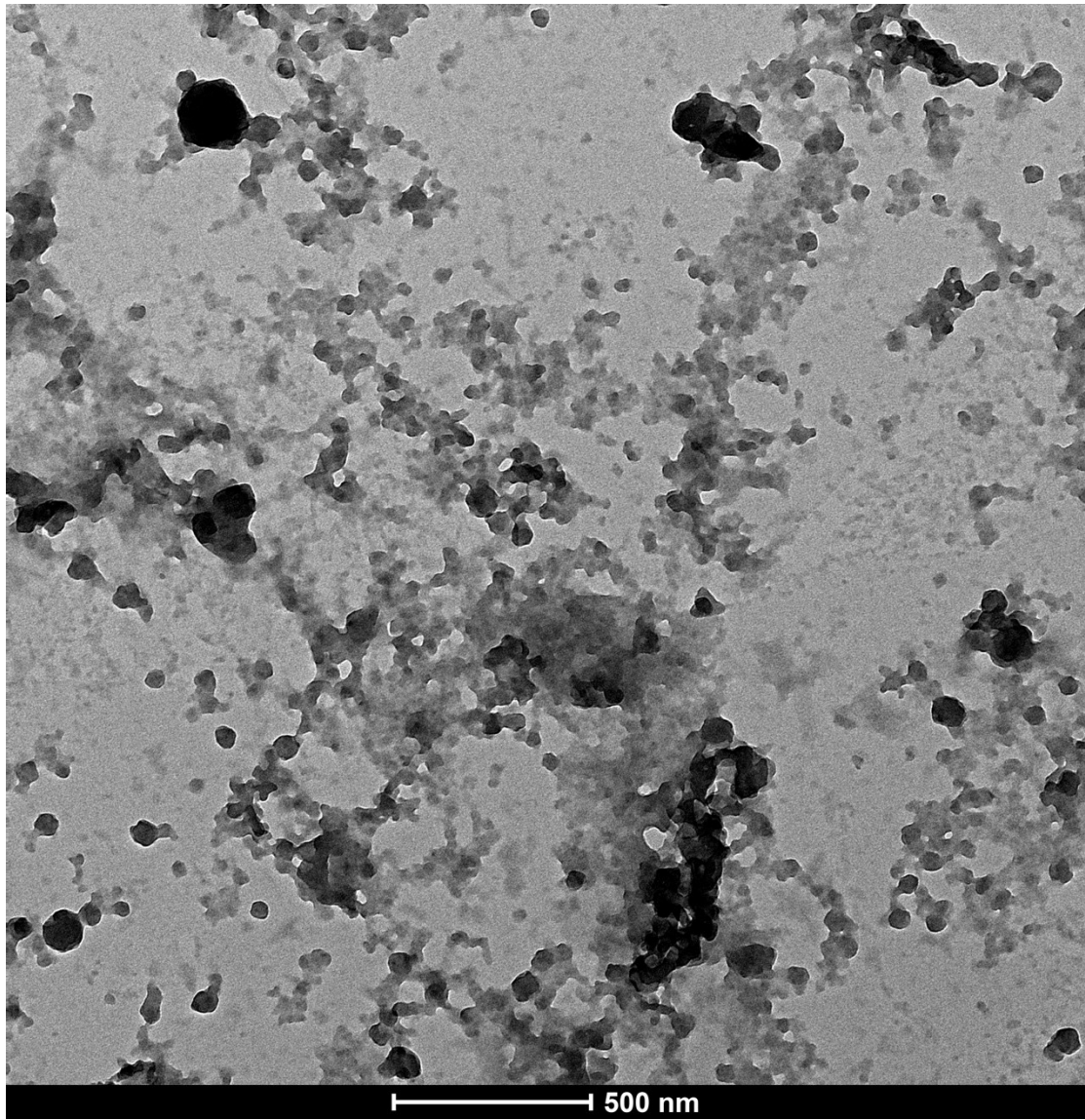


Figure S2 TEM image of PI NPs directly mixed with RBC vesicles, indicating that PI NPs and RBC vesicles rapidly co-precipitated due to the strong electrostatic interaction.

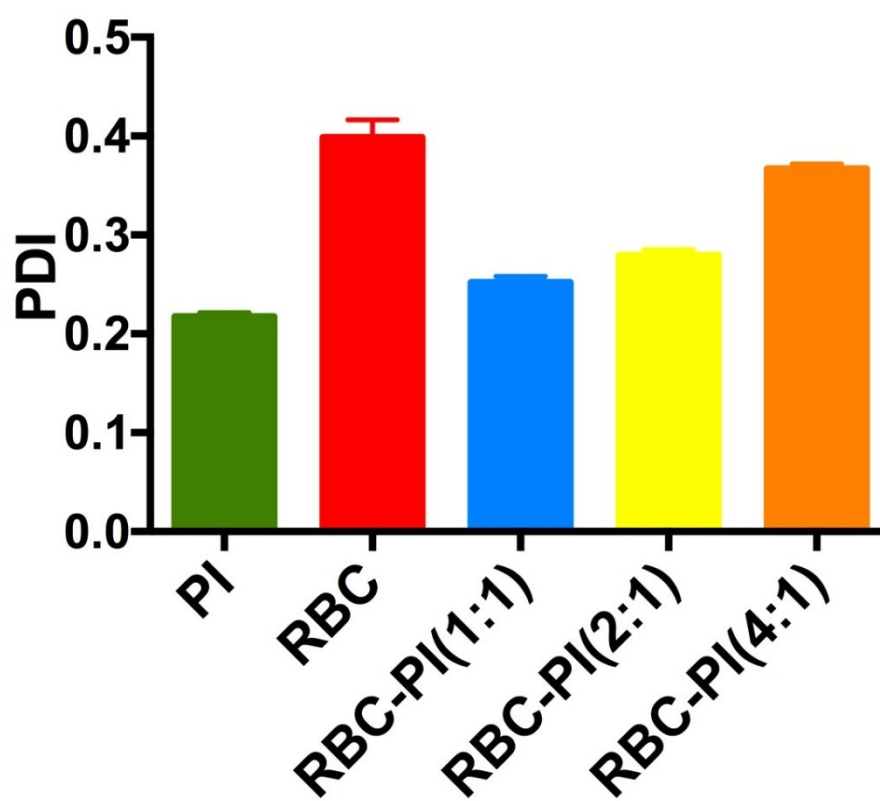


Figure S3 Polydispersity index (PDI) of the RBC vesicles to PI complexed nanoparticles at different ratios.

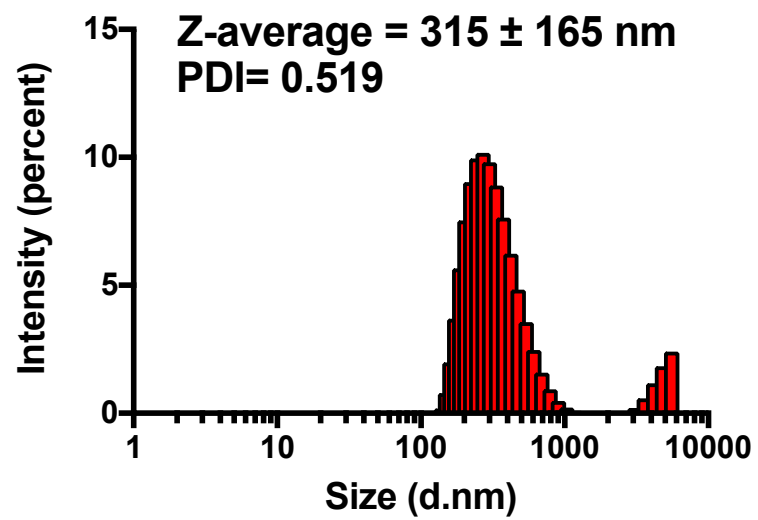


Figure S4 DLS measurements of the size (intensity) of RBC-PI (0.5:1).

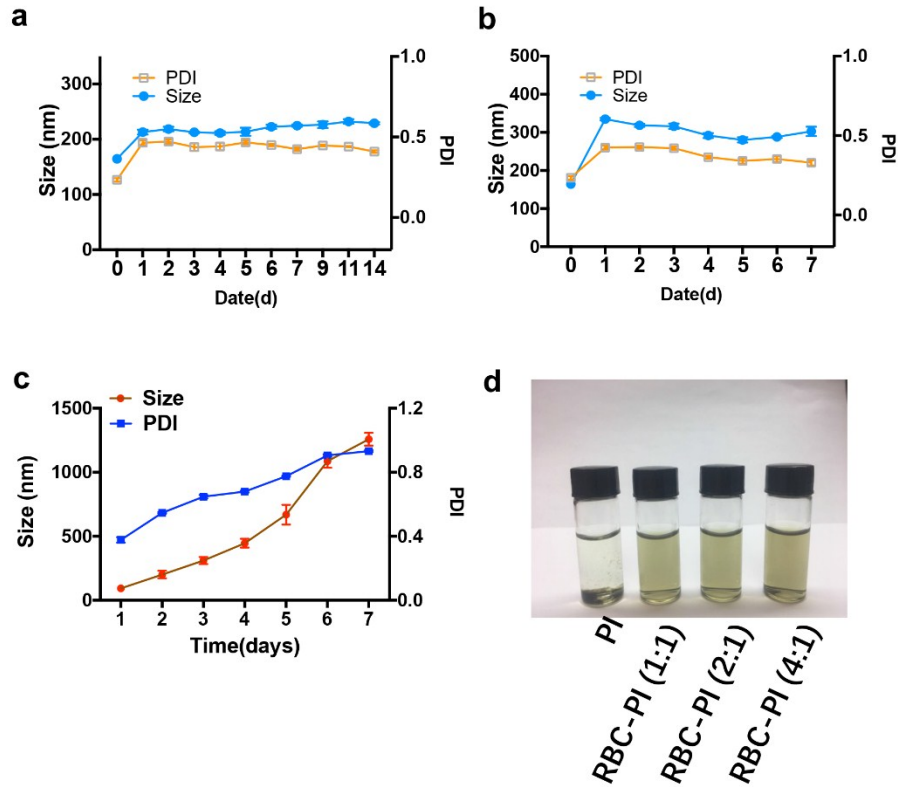


Figure S5 Stability test of RBC-PI in the presence of a) 100% FBS and b) 100% homologous human serum. Nanoparticle size and PDI were measured by DLS over 14 and 7 days, respectively. c) Aggregation of PI NPs evaluated by light dynamic scattering (DLS). 1 mg/mL PI NPs were incubated with 10% fetal bovine serum additions. The materials were incubated in a cell incubator, which provided 10% humidity, 5% CO₂ and 37 °C incubating temperature. d) 5 µg/mL PI and various RBC vesicles-to-PI ratios dispersed in 10% FBS PBS solution after 30 days; PI were precipitated due to the ostwald ripening.

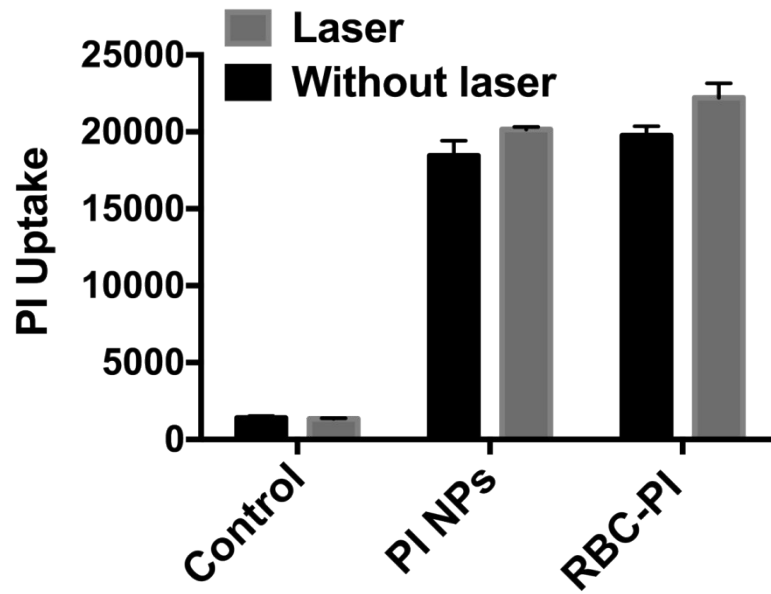


Figure S6 Intracellular cell uptake of PI NPs and RBC-PI with and without light treatment assessed with flow cytometry.

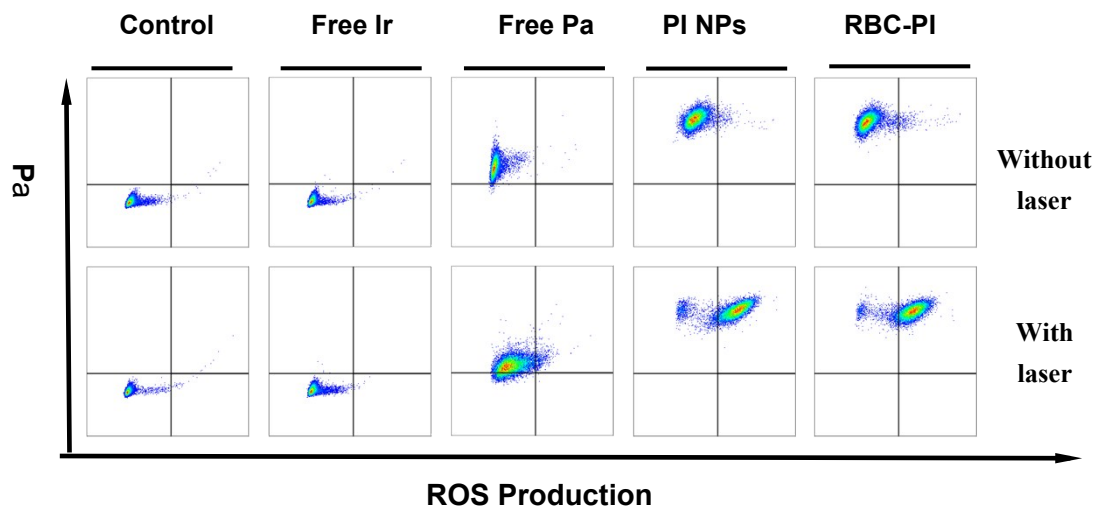


Figure S7 FACS quantitatively exhibited the ROS production of PI NPs and RBC-PI in A549 cells. The ROS production indicated by DCF-DA with FITC channel (x-axis), Pa denoted the fluorescence of PI with Cy5.5 channel (y-axis).

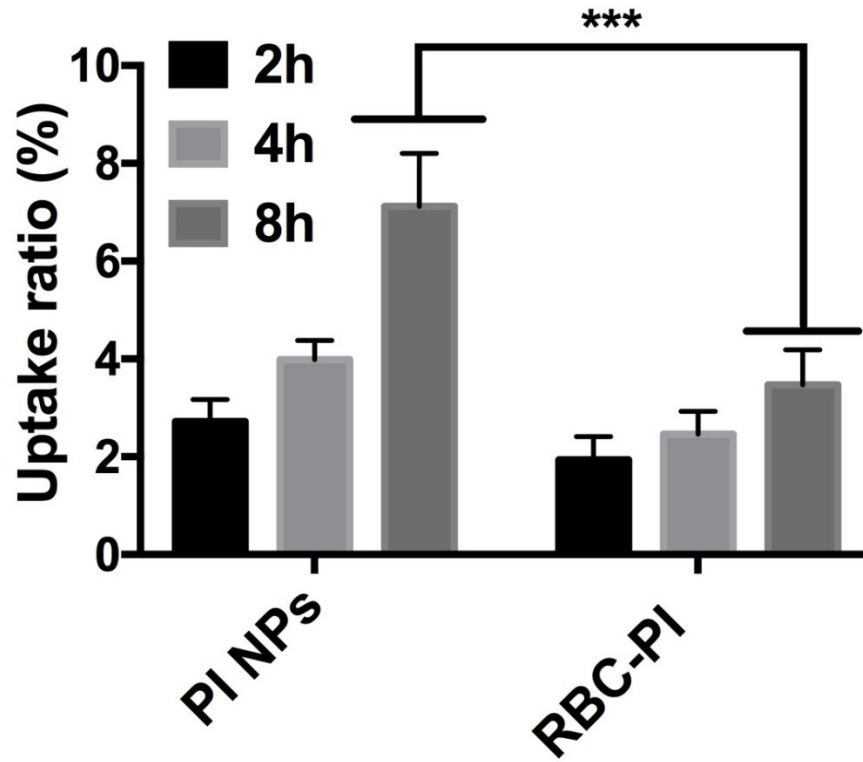


Figure S8 Intracellular uptake of RBC-PI and PI NPs in RAW267.4 cells after 2, 4, 8 h incubation. (***) $P < 0.0001$.

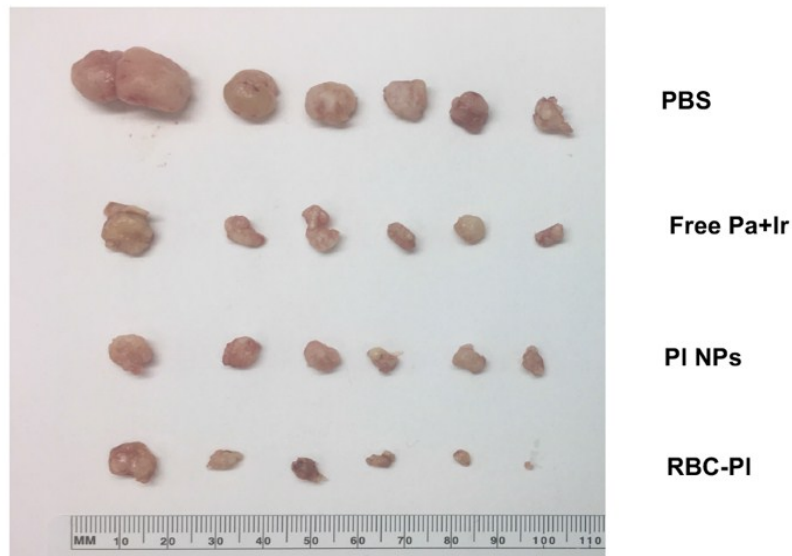


Figure S9 The size of collected tumors from mice with different treatment groups. The mice were treated with free Pa+Ir, PI NPs and RBC-PI, respectively. PBS treated group was set as control. All groups were treated with laser (1.2 W/cm^2) for 3 min in tumor site.

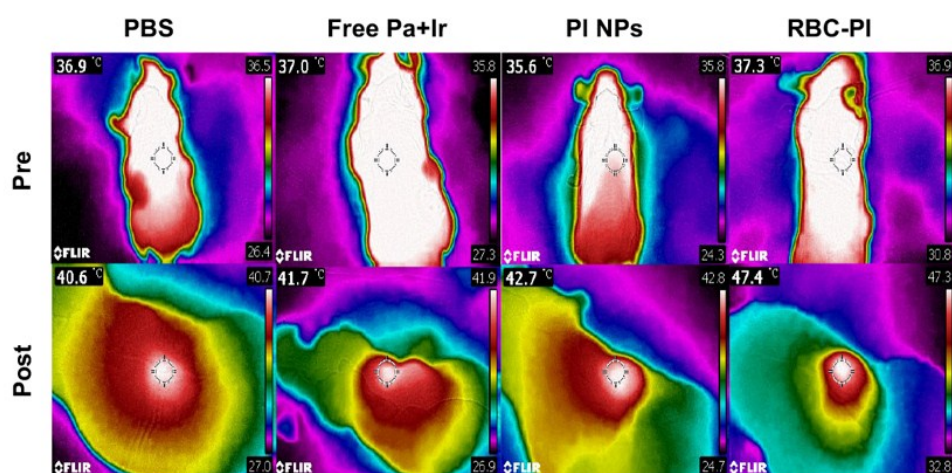


Figure S10 Photothermal effect of Pa+Ir, PI NPs and RBC-PI groups; the photos were recorded by a thermal imaging camera.

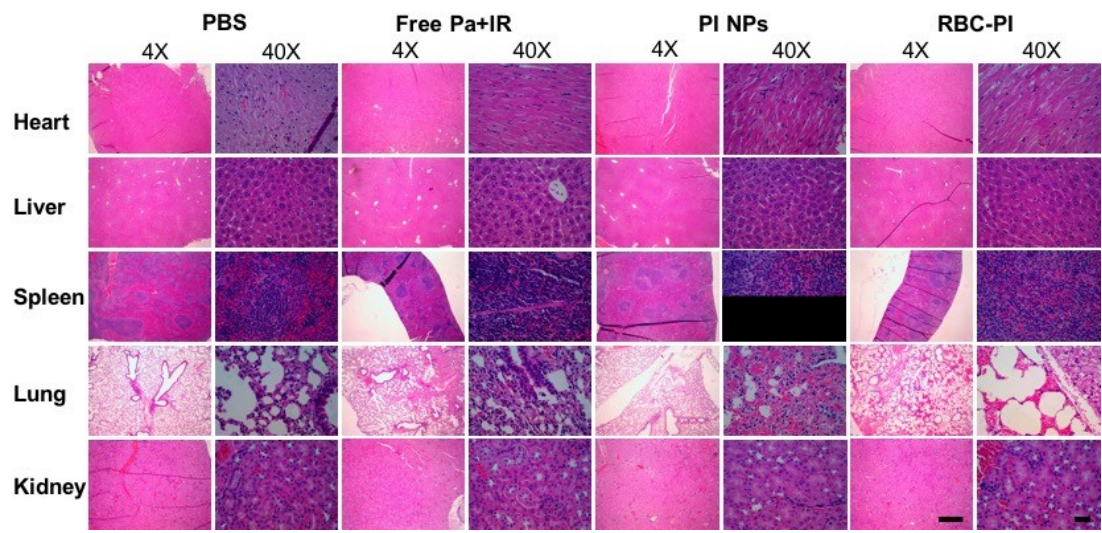


Figure S11 Hematoxylin and eosin (H&E) staining of the organs after different treatments, bar= 200 μm for 4 \times , bar= 60 μm for 40 \times .

Table S1 Pharmacokinetics parameters of RBC-PI and PI NPs.

Parameters	Unit	RBC-PI	PI NPs
AUC(0-t)	ug/L*h	58824.6±71.9	5902.7±181.2
Cmax	ug/L	11243.3±243.6	1146.4±215.4
Tmax	h	0.5±0.2	0.25±0.2
t1/2	h	17.3± 2.5	9.1± 2.7